NUMERICAL INVESTIGATION OF THE INFLUENCE OF REINFORCEMENT CONFIGURATION ON CONSTRUCTION RESPONSE OF REINFORCED SOIL SEGMENTAL WALLS

Kianoosh Hatami, Associate Research Director, GeoEngineering Centre at Queen's-RMC, Department of Civil Engineering, Royal Military College of Canada, Kingston, Ontario
Richard J. Bathurst, Professor, GeoEngineering Centre at Queen's-RMC, Department of Civil Engineering, Royal Military College of Canada, Kingston, Ontario

ABSTRACT
The paper describes the verification of a numerical model that has been developed using the program FLAC to simulate the response of geosynthetic reinforced soil retaining walls constructed with a modular concrete block (segmental) facing. The numerical results are compared to physical measurements taken from four full-scale (i.e. 3.6 m-high) reinforced soil walls that were constructed with different arrangements of a biaxial polypropylene (PP) geogrid reinforcement in an in-doors test facility. All wall components and construction procedures were otherwise identical. The walls were extensively instrumented and monitored with more than 300 instrumentation points. It is shown that for all four test walls, the predicted responses for a wide range of external and internal wall response parameters are in satisfactory agreement with the measured data. The effect of reinforcement spacing and stiffness on wall response at end of construction was detected in the test walls examined. However, It was found that the stiff structural facing of the test walls reduced the sensitivity of the wall response to variations in reinforcement configuration.

RÉSUMÉ
L'article décrit la vérification d'un modèle numérique qui fût développé avec le programme FLAC pour simuler la réponse de murs en terre armée de géosynthétiques, construits avec un parement modulaire en blocs de béton. Les résultats numériques sont comparés à des mesures physiques tirées de nos murs à grande échelle (3.6 m de haut), construits avec différents agencements d'une géogrille biaxiale de polypropylène dans une installation d'essai intérieure; toutes autres composantes et modes de construction des murs furent identiques. Les murs ont été fortement instrumentés et surveillés à l'aide de plus de 300 points de mesure. On montre que pour les quatre murs, les réponses prédites pour un éventail étendu de paramètres de réponse interne et externe des murs sont en accord satisfaisant avec les données mesurées. L'effet de l'espacement et de la rigidité des armatures sur la réponse du mur en fin de construction fût détectée pour les murs d'essai étudiés. Cependant, on a observé que le parement structural rigide des murs d'essai a réduit la sensibilité de la réponse du mur aux variations dans la configuration de l'armature.

1. INTRODUCTION

1.1 Background

Recent studies have shown that current North American design practice for geosynthetic reinforced soil (GRS) walls (AASHTO 2002, Elias et al. 2001) is excessively conservative (e.g. Allen et al. 2002). Allen and Bathurst (2002) pointed out that current limit equilibrium-based approaches need to be replaced by more advanced design methodologies that are based on better understanding of the mechanical response of GRS walls subjected to different loading conditions. The writers and co-workers have been engaged in a long-term research undertaking that involves the construction and monitoring of carefully instrumented large-scale geosynthetic reinforced soil retaining walls built within a controlled laboratory environment (Bathurst et al. 2000, 2001). This on-going research programme is aimed at generating high-quality and comprehensive data that can be used to verify advanced numerical models of geosynthetic reinforced soil walls. The models can then be used to extend the limited database of laboratory and field case studies to a wider range of reinforced soil wall types, component materials and configurations. The combination of physical and numerical test results can subsequently be used to check or refine recently proposed analytical design methods for geosynthetic reinforced soil wall structures that hold promise to make these systems more cost effective (e.g. Allen et al. 2003).

1.2 Current study

The focus of this paper is on the development of a numerical model and its validation using the measured response of four well-instrumented large-scale test walls constructed in the RMC retaining wall test facility. These walls were identical with the exception of reinforcement spacing or stiffness value. A FLAC (Itasca 2001) numerical model was developed to predict the performance of the test walls up to the end of construction, which represents a working stress

(i.e. serviceability) condition that is of most interest to designers. The paper describes the four physical test walls that were simulated numerically and provides details of the constitutive models used for the component materials in the walls. Numerical results are compared to measured horizontal and vertical toe boundary reactions, vertical earth pressures at the foundation, facing horizontal displacements, connection loads, and reinforcement strain distributions. However, for brevity, only selected output results are presented in this paper.

2. PHYSICAL TEST WALL MODELS

Figure 1a shows a schematic cross-sectional view of Wall 1 (control wall) with a modular block (segmental) facing and six reinforcement layers. All test walls were 3.6 m high with a target facing batter of 8° from the vertical.

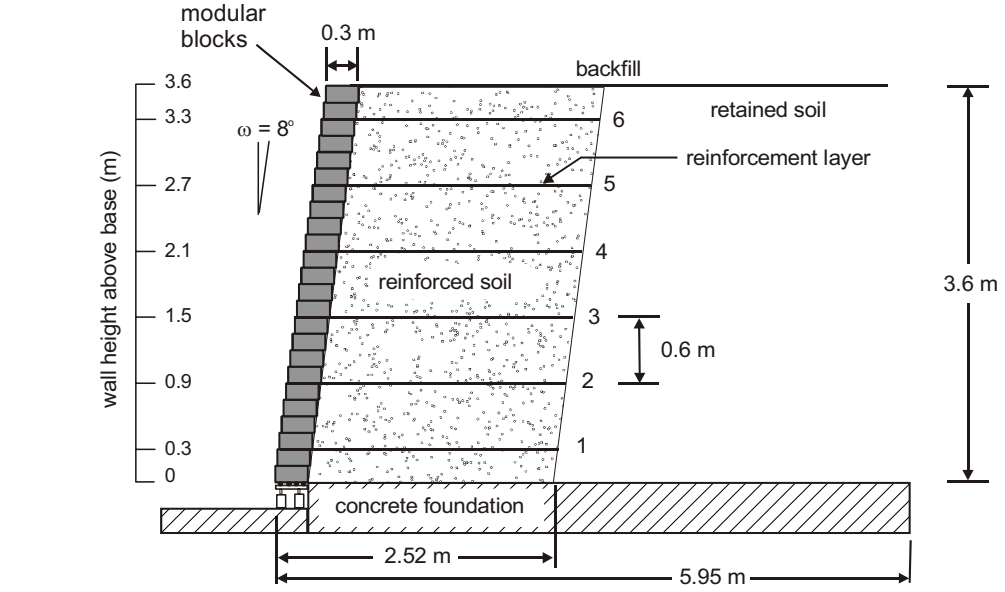

a)

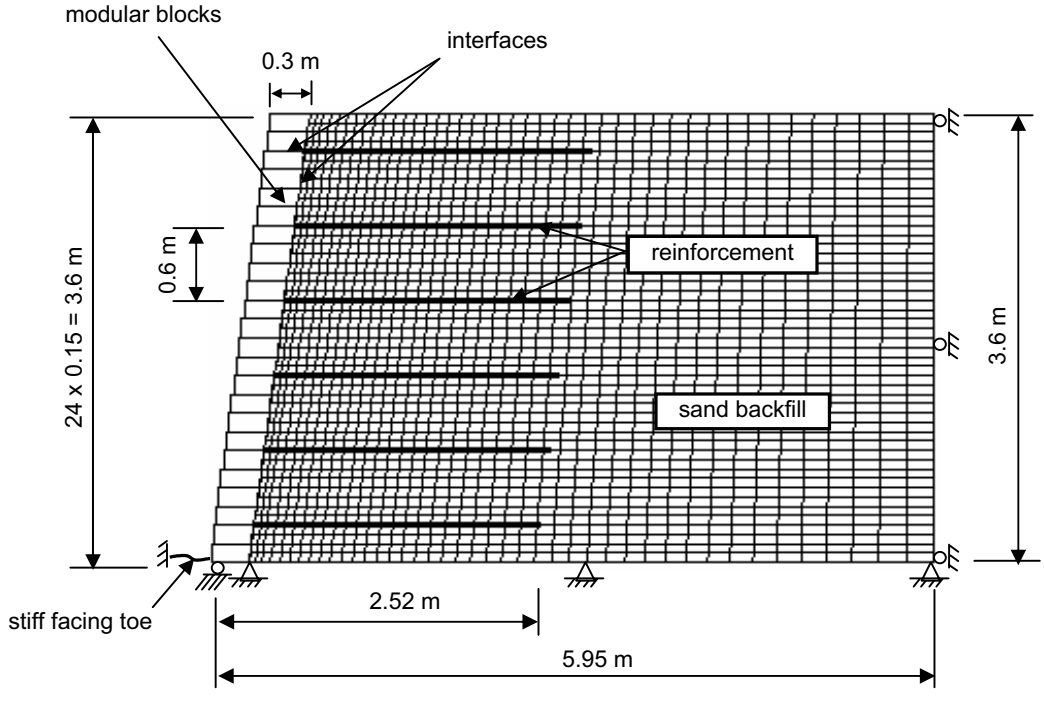

b)

Figure 1. Cross-section view of Wall 1 (control structure) with six layers of reinforcement: (a) Schematic view of basic components; (b) FLAC numerical model

The reinforcement was a weak bi-axial polypropylene (PP) geogrid material. Wall 2 was built with a PP reinforcement that had 50% of the stiffness and strength of the reinforcement used in Wall 1 but was otherwise identical to Wall 1. Walls 3 and 7 (from a set of eleven test walls) were nominally identical to Wall 1 except that only four and eleven reinforcement layers were used in these walls at vertical spacing values of 0.9 m and 0.3 m, respectively. The values of global index reinforcement stiffness of the four walls - defined as (Christopher et al. 1990, Allen et al. 2003):

$$S_{index} = \frac{J_{ave}}{(H/n)} = \frac{\sum_{i=1}^{n} J_i}{H} \quad (1)$$

are given in Table 1. In Equation 1, J_{ave} is the average index tensile stiffness of all (n) reinforcement layers over the wall height, H, and, J_i is the secant tensile stiffness of an individual reinforcement layer taken at 2% strain as measured in a wide-width strip tensile test in accordance with ASTM D4595. According to Table 1, Wall 7 and Wall 2 are the stiffest and the least stiff walls discussed here, respectively.

In each structure, the wall facing was built with three discontinuous vertical sections (columns) with separate reinforcement layers in plan view. Each facing column comprised of 300 mm-wide (toe to heel) by 150 mm-high by 200 mm-long masonry concrete blocks. The solid units transfer shear between courses through a continuous shear key. Vertical joints were used to isolate the 1 m - wide instrumented centre column. The discontinuous wall facing and reinforcement layers together with a sidewall friction reduction treatment were used to minimize the frictional effects of the lateral boundaries of the test facility and allow the instrumented middle section of the wall structure to approach a plane strain test condition as far as practical.

The backfill was a clean, uniform-size rounded beach sand (SP) with fines content less than 1%. The sand had a flat compaction curve which enabled the final compacted density to be essentially uniform through the entire backfill. The sand was placed in 150 mm lifts matching the height of the facing units and compacted using either a lightweight vibrating plate compactor (Walls 1,2 and 3) or a jumping jack (Wall 7). The soil within 1 m of the facing column was compacted to the same target density using a hand-operated plate compactor. The measured backfill dry unit weight and moisture content were 16.3 ± 0.4 kN/m^3 and 3%, respectively. A bulk unit weight of 16.8 kN/m^3 was used in the numerical simulations. The reinforcement layers in the wall middle section were rigidly attached to the facing using mechanical connections. This arrangement prevented reinforcement slippage between the facing blocks and thereby simplified the measurement and interpretation of connection loads.

Table 1. Reinforcement stiffness and strength properties of polypropylene geogrid[1]

Wall No.	Number of layers	Vertical spacing S_v (m)	Global index stiffness S_{index} (kN/m^2)[2]
1	6	0.6	476
2	6	0.6	238
3	4	0.9	318
7	11	0.3	524

Notes:
(1) strain-dependent tangent stiffness of reinforcement, J_t, is determined from Equation 2; yield strength, T_y, based on peak strength measured during 10%/min constant-rate-of-strain (CRS) test (ASTM D4595) is 12 kN/m.
(2) from Equation 1

Table 2. Material properties for sand backfill

Stiffness properties (Hyperbolic model[1])	Problem configuration	
	Axisymmetric (Triaxial)	Plane strain[2]
K_e (elastic modulus number)	510	1150, 2840[3]
K_b (bulk modulus number)	575	575, 1420[3]
K_{ur} (unloading-reloading modulus number)	612[4]	1380[4], 3410[3,4]
n (elastic modulus exponent)	0.5	0.5
m (bulk modulus exponent)	0.5	0.5
R_f (failure ratio)	0.86	0.86
ν_t (tangent Poisson's ratio)	-	0 - 0.49
Strength properties		
ϕ (peak friction angle) (^{o})	40	44
c (cohesion) (kPa)	0	1
ψ (dilation angle) (^{o})	11	11
Bulk unit weight of backfill		
γ (kN/m^3)	-	16.8

Notes:
(1) Duncan et al. (1980)
(2) values used in FLAC numerical model for sand backfill in Walls 1 to 3 unless otherwise stated
(3) values for Wall 7
(4) assumed 1.2K_e for compacted sand (Duncan et al. 1980)

3. NUMERICAL MODEL AND MATERIAL PROPERTIES

The finite difference-based program Fast Lagrangian Analysis of Continua - FLAC (Itasca 2001) was used to develop the numerical model for the reinforced soil test walls and to simulate their plane strain response during and at the end of construction. The backfill and facing modular blocks were modelled with continuum zones and reinforcement layers were modelled with structural elements. The wall foundation in the numerical model was assumed to be rigid, which modelled the rigid concrete foundation (strong floor) of the RMC test facility. Figure 1b shows the numerical grid used for the segmental retaining walls. The mesh size and maximum unbalanced force at the grid points (i.e. error tolerance) were selected based on a series of parametric analyses to concurrently optimize accuracy and computation speed.

Numerical computations were carried out in large-strain mode to ensure sufficient accuracy in the event of large wall deformations or reinforcement strains and to accommodate the moving local datum as each row of facing units and soil layer was placed over the previous numerical grid during construction simulation.

The compacted backfill was modelled as a homogenous, isotropic, nonlinear elastic-plastic material with Mohr-Coulomb failure criterion and dilation angle (non-associated flow rule), with the plane strain material properties shown in Table 2. Wall 7 was built with a heavier compactor than the compactor used in Walls 1, 2 and 3. Therefore, greater backfill modulus numbers were back calculated for Wall 7 from load-settlement results during surcharge loading of the walls after construction.

The reinforcement layers were modelled using two-noded elastic-plastic cable elements with strain-dependent tangential tensile stiffness, $J_t(\varepsilon)$, tensile yield strength, T_y and no compressive strength. The measured load-strain response of the PP reinforcement from an in-isolation, constant-rate-of-strain (CRS) test at 0.01% strain/min was used to determine the equation for $J_t(\varepsilon)$ over the strain range observed during the construction stage of the walls (i.e. $\varepsilon < 1.5\%$) as:

For Walls 1, 3 and 7:

$$J_t(\varepsilon) = \frac{dT}{d\varepsilon} = 119 - 2938\varepsilon \quad (2)$$

For Wall 2:

$$J_t(\varepsilon) = \frac{dT}{d\varepsilon} = 59.5 - 1469\varepsilon \quad (3)$$

where T is axial load and ε is axial strain.

The interfaces between dissimilar materials were modelled as linear spring-slider systems with interface shear strength defined by the Mohr-Coulomb failure criterion. Interface stiffness values in normal (k_n) and tangential (k_s) directions were initially selected using the recommended rule-of-thumb estimates given by Itasca (2001). However, the interface stiffness values were adjusted by comparing them with values from physical test data (if available) and/or refining the magnitude of k_n and k_s to avoid intrusion of adjacent zones (a numerical effect) and to prevent excessive computation time. Final interface property values used in the numerical simulations of all model walls are summarized in Table 3. Compaction of sand backfill was simulated by applying a uniform vertical stress (equal to 8 kPa in Walls 1, 2 and 3 and 16 kPa in Wall 7) to the entire surface of each new backfill layer as the wall was constructed from the bottom-up before solving the model to equilibrium. Further details of the numerical model are given by Hatami and Bathurst (2004).

Table 3. Interface properties

Soil-block	Value
δ_{sb} (friction angle) (^{o})	44
ψ_{sb} (dilation angle) (^{o})	11
k_{nsb} (normal stiffness) (MN/m/m)	100
k_{ssb} (shear stiffness) (MN/m/m)	1
Block-block	
δ_{bb} (friction angle) (^{o})	57
c_{bb} (cohesion) (kPa)	46
k_{nbb} (normal stiffness) (MN/m/m)	1000
k_{sbb} (shear stiffness) (MN/m/m)	50

4. RESULTS

The response results for each of the four test walls in this study were obtained by changing the reinforcement spacing or stiffness values between the wall models to match the corresponding physical test (Table 1). The remaining material properties for all wall components were kept the same.

Figure 2 shows the histories of measured and calculated horizontal and vertical toe loads for the walls during construction. The histories of predicted and recorded toe loads are in overall close agreement. Variation of the weight of the middle facing column with wall height during construction for each wall is also shown in Figure 2. It is seen that the total vertical toe load is greater than the column self-weight due to down-drag forces generated by relative vertical settlement of the sand backfill with respect to the reinforcement-wall connections as the walls rotate outward during construction. Both physical and numerical results for all four walls indicated that reinforcement spacing or stiffness value has a negligible effect on the magnitude of toe loads during construction for the wall height, facing type and reinforcement configurations examined.

Figure 3 shows the measured (average, minimum and maximum values of each pair of instruments at each

reinforcement elevation) and numerically calculated displacement values at end of construction. The measured displacement results are readings from pairs of potentiometers that were mounted against the facing blocks during construction. Therefore, the recorded displacement value at each elevation in the figure represents the magnitude of the lateral displacement of the corresponding facing block from the time of placement (i.e. after mounting the potentiometer) to the end of construction. Hence, these plots should not be confused with the actual wall deformation profiles at the end of construction. The results in Figure 3 show satisfactory agreement between the maximum recorded and predicted lateral displacements for each wall and the general trend in the data. Wall 2 (the wall with the lowest global index reinforcement stiffness value) gave the largest maximum displacement based on both experimental and numerical results. However, from a practical point of view, the differences are insignificant (i.e. numerical results for maximum displacements are within 1 mm). The relatively large facing displacement of Wall 7 with eleven reinforcement layers is attributed to the greater compaction effort imparted during construction compared to the compaction effort applied to the other three walls.

Figure 4 shows the measured and predicted reinforcement strain distributions in the test walls at end of construction. The measured results are data from strain gauge readings and strains deduced from extensometers. Included with the physical measurements are error bars representing ±1 standard deviation from the mean strain value of strain gauge pairs mounted at the same distance from the back of the facing column but on different parallel longitudinal geogrid members. A similar reliability estimate is plotted for strains deduced from extensometer points distributed along the length of each instrumented reinforcement layer.

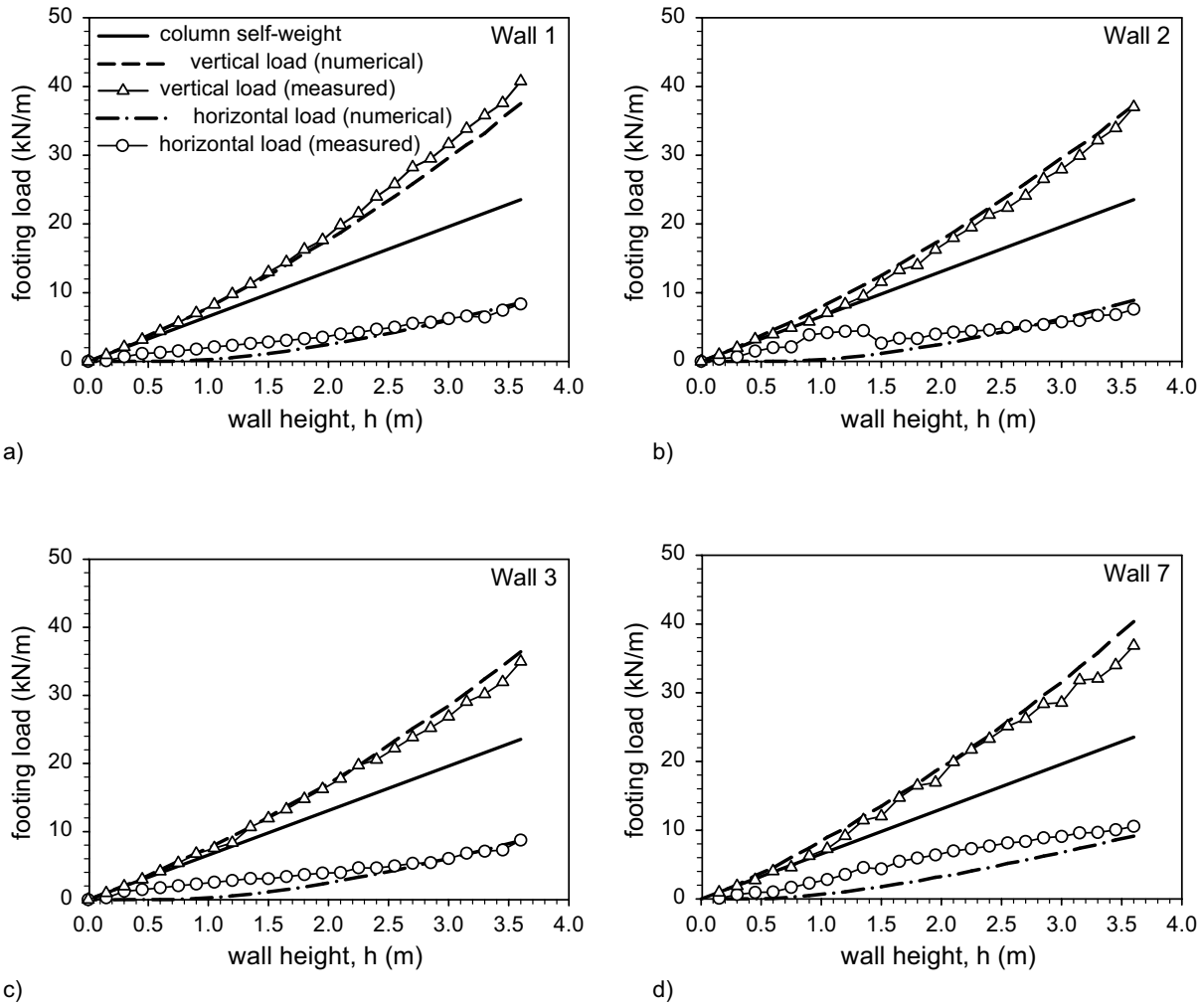

Figure 2. Horizontal and vertical toe loads at base of facing column in Walls 1, 2, 3 and 7

The magnitude of variability in strain estimates is based on values reported by Bathurst et al. (2002) who quantified the accuracy of strain readings as a function of strain level and instrumentation type. Based on the accuracy of strain measurements and taking all four walls and 27 instrumented layers into consideration, the numerically predicted strain readings are judged to be in good agreement. For example, in most cases, the peak strain magnitudes from strain gauge readings are close and for many layers, the sharp strain gradient in the vicinity of the connections is captured. Differences in magnitude of strain values (measured and predicted) are difficult to detect between the four walls despite differences in global index reinforcement stiffness values that vary by a factor of 2.2. (Section 2 and Table 1). This observation can be understood by recognizing the contribution of the stiff facing column in combination with the restrained toe boundary condition to transmitting lateral earth forces to the foundation.

5. CONCLUSIONS

A numerical model has been developed to predict the response of geosynthetic reinforced soil modular block retaining walls during construction. The predicted wall response results from the plane strain numerical models are compared with the measured response of four 3.6 m-high test walls constructed with a sand backfill and different geogrid reinforcement configurations. The numerical model accounts for staged construction of the segmental retaining walls including backfill compaction and incremental lateral displacement of the modular facing during construction. The numerical model also includes a stress-dependent model for backfill stiffness properties and a strain-dependent axial stiffness for the reinforcement. Predicted results were shown to be in generally good agreement with measured data including toe loads, wall deformations and reinforcement strains.

A unique feature of this study is that a wide range of response parameters were predicted for four nominally identical walls in which only the reinforcement configuration was varied and compaction effort adjusted in accordance with the physical tests. All other component material properties were kept identical as determined from careful examination and interpretation of independent test results for the component materials. The segmental test walls investigated had a stiff structural facing and their maximum vertical reinforcement spacing was less than three times the width of the facing blocks. As a result, the effect of reinforcement configuration on the end-of-construction response of the walls examined was found to be insignificant.

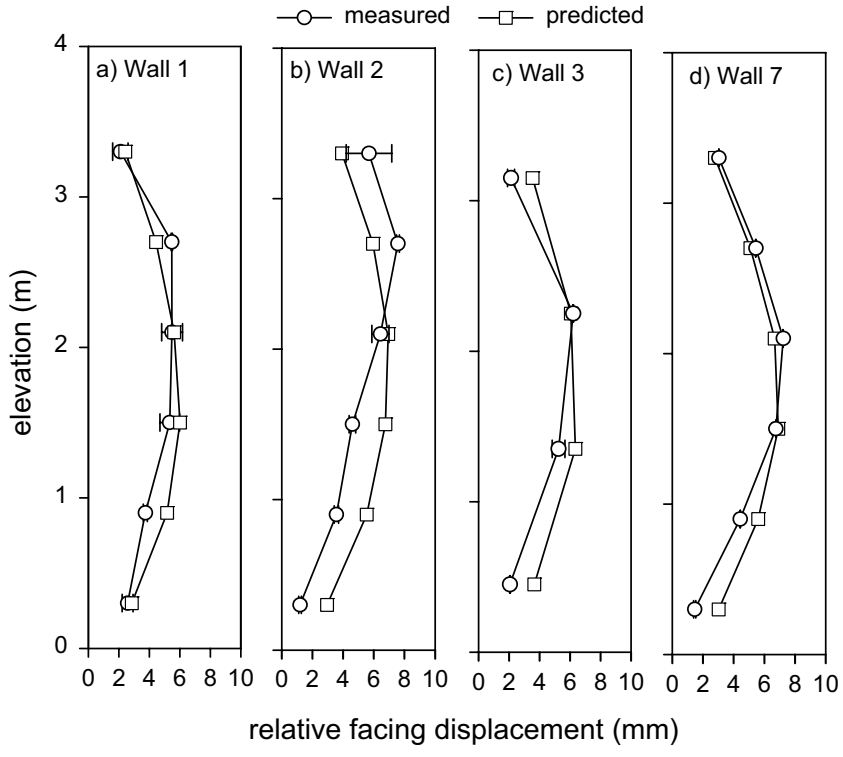

Figure 3. Relative wall facing displacements measured at reinforcement elevations. Note: Error bars represent range of deflection reading using two displacement potentiometers at each elevation.

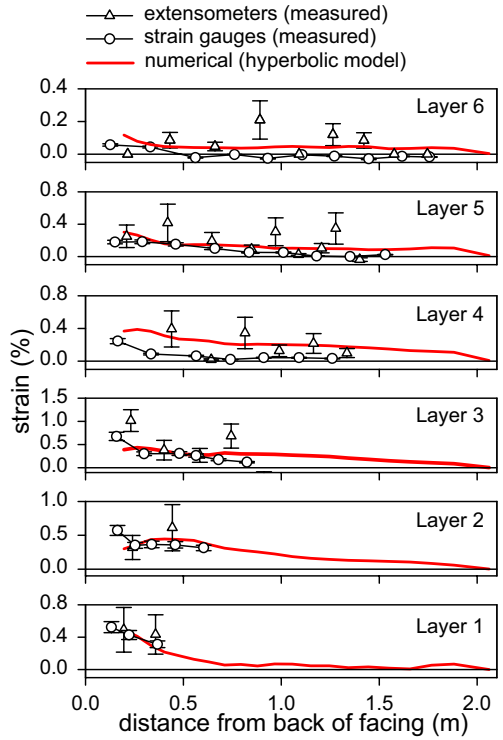

a) Wall 1 (6 layers)

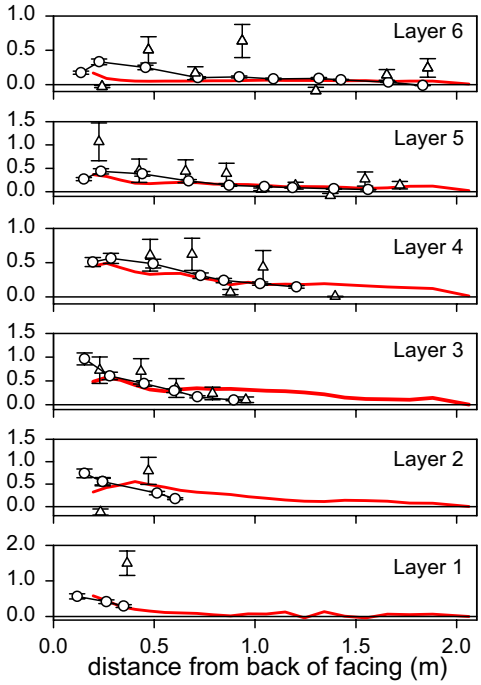

b) Wall 2 (6 layers)

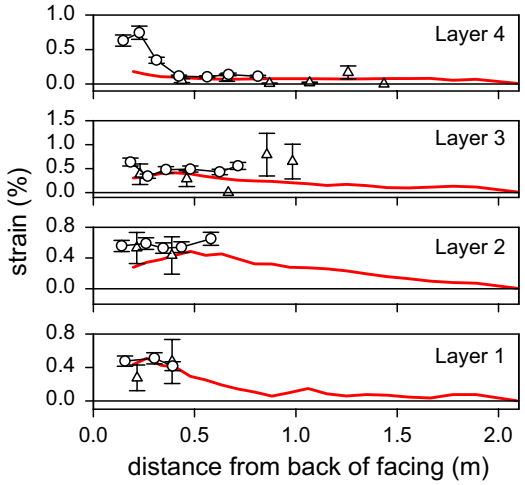

c) Wall 3 (4 layers)

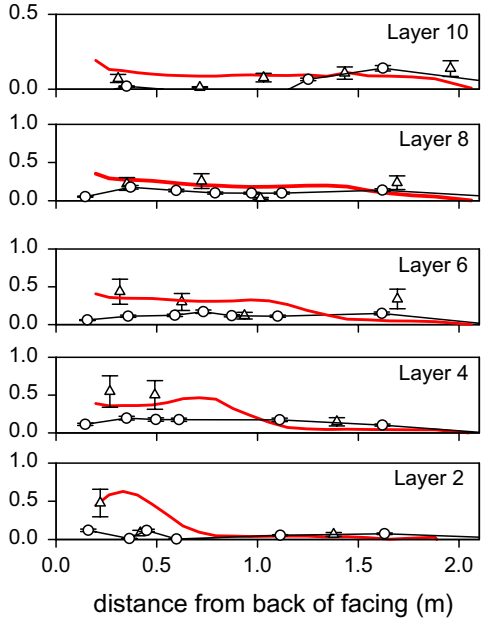

d) Wall 7 (11 layers)

Figure 4. Magnitude and distribution of measured and predicted reinforcement strains: Note: Error bars represent ± one standard deviation on estimated strain values.

ACKNOWLEDGEMENTS

The financial support for this study was provided by the Natural Sciences and Engineering Research Council (NSERC) of Canada and the following US State Departments of Transportation: Washington, Alaska, Arizona, California, Colorado, Idaho, Minnesota, New York, North Dakota, Oregon, Utah, and Wyoming. The writers are also grateful for the financial support from the RMC Academic Research Program and operating grants from the Department of National Defence, Canada. Contributions of P. Burgess, N. Vlachopoulos and K. P. LeBlanc (former graduate students) who carried out the physical model tests described in this paper are acknowledged.

REFERENCES

Allen, T.M. & Bathurst, R.J. 2002. Soil reinforcement loads in geosynthetic walls at working stress conditions. Geosynthetics International, 9(5-6): 525-566.

Allen, T.M., Bathurst, R.J. & Berg, R.R. 2002. Global level of safety and performance of geosynthetic walls: A historical perspective. Geosynthetics International, 9(5-6): 395-450.

Allen, T.M., Bathurst, R.J., Lee, W. F., Holtz, R.D. & Walters, D.L. 2003. A new working stress method for prediction of reinforcement loads in geosynthetic walls. Canadian Geotechnical Journal, 40: 976-994.

ASTM D4595. Standard test method for tensile properties of geotextiles by the wide-width strip method (D4595-86). 1996 Annual book of ASTM standards. American Society for Testing and Materials (ASTM), West Conshohocken, Pa., USA, 4.09: 698-708.

AASHTO. 2002. Standard specifications for highway bridges. 17th ed. American Association of State Highway and Transportation Officials, Washington, DC, USA.

Bathurst, R.J., Allen, T.M. & Walters, D.L. 2002. Short-term strain and deformation behaviour of geosynthetic walls at working stress conditions, Geosynthetics International, 9(5-6): 451-482.

Bathurst, R.J., Walters, D.L., Hatami K. & Allen. T.M. 2001. Full-scale performance testing and numerical modelling of reinforced soil retaining walls, Special plenary lecture: International Symposium on Earth Reinforcement, IS Kyushu 2001, Fukuoka, Japan, November 2001, 2: 777-799.

Bathurst, R.J., Walters, D., Vlachopoulos, N., Burgess, P. & Allen, T.M. 2000. Full scale testing of geosynthetic reinforced walls, Invited keynote paper, ASCE Special Publication No. 103, Advances in Transportation and Geoenvironmental Systems using Geosynthetics, Proceedings of Geo-Denver 2000, August 2000, Denver, CO, USA, 201-217.

Christopher, B.R., Gill, S.A., Giroud, J.-P., Juran, I., Mitchell, J.K., Schlosser, F. & Dunnicliff, J. 1990. Reinforced Soil Structures Vol. 1: Design and Construction Guidelines. FHWA Report FHWA-RD-89-043, USA.

Duncan, J.M., Byrne, P., Wong, K.S. & Mabry, P. 1980. Strength, stress-strain and bulk modulus parameters for finite-element analysis of stresses and movements in soil masses, Report No. UCB/GT/80-01, Department of Civil Engineering, University of California, Berkeley, CA, USA.

Elias, V., Christopher, B.R., & Berg, R.R. 2001. Mechanically stabilized earth walls and reinforced soil slopes - design and construction guidelines. FHWA-NHI-00-043, Federal Highway Administration, Washington, DC, USA.

Hatami, K. & Bathurst, R.J. 2004. Development and verification of a numerical model for the analysis of geosynthetic reinforced-soil segmental walls. (submitted to Canadian Geotechnical Journal).

Itasca Consulting Group. 2001. FLAC - Fast Lagrangian Analysis of Continua, v 4.00, Itasca Consulting Group Inc., Minneapolis, MN, USA.